Flow Facility Design and Experimental Studies of Wall-Bounded Turbulent Shear-Flows

by

Björn Lindgren

December 2002
Technical Reports from
Royal Institute of Technology
Department of Mechanics
SE-100 44 Stockholm, Sweden

Typsatt i $\mathcal{AMS}$-LaTeX med mekaniks avhandlingsstil.

Akademisk avhandling som med tillstånd av Kungliga Tekniska Högskolan i Stockholm framlägges till offentlig granskning för avläggande av teknologie doktorsexamen tisdagen den 17:e december 2002 kl 10.15 i Kollegiesalen, Administrationsbyggnaden, Kungliga Tekniska Högskolan, Valhallavägen 79, Stockholm.

Edita Norstedts tryckeri, Stockholm 2002

Björn Lindgren 2002 **Flow facility design and experimental studies of wall-bounded turbulent shear-flows**

Department of Mechanics, Royal Institute of Technology
SE-100 44 Stockholm, Sweden

Abstract

The present thesis spans a range of topics within the area of turbulent flows, ranging from design of flow facilities to evaluation of scaling laws and turbulence modeling aspects through use of experimental data. A new wind-tunnel has been designed, constructed and evaluated at the Dept. of Mechanics, KTH. Special attention was directed to the design of turning vanes that not only turn the flow but also allow for a large expansion without separation in the corners. The investigation of the flow quality confirmed that the concept of expanding corners is feasible and may be successfully incorporated into low turbulence wind-tunnels. The flow quality in the MTL wind-tunnel at the Dept. of Mechanics, KTH, was also investigated confirming that it still is very good. The results are in general comparable to those measured when the tunnel was new, with the exception of the temperature variation that has decreased by a factor of 4 due to an improved cooling system.

Experimental data from high Reynolds number zero pressure-gradient turbulent layers have been investigated. These studies have primarily focused on scaling laws with *e.g.* confirmation of an exponential velocity defect law in a region, about half the size of the boundary layer thickness, located outside the logarithmic overlap region. The streamwise velocity probability density functions in the overlap region was found to be self-similar when scaled with the local rms value. Flow structures in the near-wall and buffer regions were studied and *e.g.* the near-wall streak spacing was confirmed to be about 100 viscous length units although the relative influence of the near-wall streaks on the flow was found to decrease with increasing Reynolds number.

The separated flow in an asymmetric plane diffuser was determined using PIV and LDV. All three velocity components were measured in a plane along the centerline of the diffuser. Results for mean velocities, turbulence intensities and turbulence kinetic energy are presented, as well as for streamlines and backflow coefficient describing the separated region. Instantaneous velocity fields are also presented demonstrating the highly fluctuating flow. Results for the above mentioned velocity quantities, together with the production of turbulence kinetic energy and the second anisotropy invariant are also compared to data from simulations based on the $k-\omega$ formulation with an EARSM model. The simulation data were found to severely underestimate the size of the separation bubble.

Descriptors: Fluid mechanics, wind-tunnels, asymmetric diffuser, turbulent boundary layer, flow structures, PDFs, modeling, symmetry methods.

Preface

This thesis concerns design and calibration of flow facilities (with special attention to wind-tunnels) as well as experimental studies of wall-bounded turbulent shear-flows (zero pressure-gradient boundary layer and plane asymmetric diffuser). Modeling aspects are tested by use of the data from the diffuser experiment and new theoretical ideas emanating from Lie group symmetry methods are evaluated by use of zero pressure-gradient turbulent boundary layer data. It is based on the following papers.

Paper 1. Lindgren, B., Österlund, J. M. & Johansson, A. V. 1998 Measurement and calibration of guide-vane performance in expanding bends for wind-tunnels. Published in *Exp. in Fluids*, 24, 1998

Paper 2. Lindgren, B. & Johansson, A. V. 2002 Design and evaluation of a low-speed wind-tunnel with expanding corners. Published as a Technical Report, TRITA-MEK 2002:14

Paper 3. Lindgren, B. & Johansson, A. V. 2002 Evaluation of the flow quality in the MTL wind-tunnel. Published as a Technical Report, TRITA-MEK 2002:13

Paper 4. Österlund, J. M., Lindgren, B. & Johansson, A. V. 1999 Flow structures in zero pressure-gradient turbulent boundary layers at high Reynolds numbers. Submitted to *Eur. J. of Mech. B / Fluids*

Paper 5. Lindgren, B., Österlund, J. M. & Johansson, A. V. 2002 Evaluation of scaling laws derived from Lie group symmetry methods in zero pressure-gradient turbulent boundary layers. Submitted to *J. Fluid Mech.*

Paper 6. Lindgren, B., Johansson, A. V. & Tsuji Y. 2002 Universality of probability density distributions in the overlap region in high Reynolds number turbulent boundary layers. Submitted to *Phys. Fluids*

Paper 7. Lindgren, B. Törnblom O. & Johansson, A. V. 2002 Measurements in a plane asymmetric diffuser with 8.5° opening angle. Part I: General flow characteristics. To be submitted.

Paper 8. Törnblom O., Lindgren, B., Gullman-Strand, J. & Johansson, A. V. 2002 Measurements in a plane asymmetric diffuser with 8.5° opening angle. Part II: Comparison with model predictions for turbulence characteristics. To be submitted.

Division of work between paper authors

The papers included in this thesis have been written in collaboration with other researchers. Below follows a description of the contribution the respondent made to the different papers. Prof. Arne V. Johansson acted as supervisor and project leader in all investigations. The respondent made a major part of the writing of the papers, if not otherwise stated below.

Paper 1. This work was made by the respondent with Dr. Jens M. Österlund acting as a second supervisor introducing the respondent into the field of experiments. The respondent presented this work at the conference Wind-tunnels and wind-tunnel test techniques, Cambridge, UK, 1997, and a written contribution was included in the conference proceedings.

Paper 2. The work in this paper was performed by the respondent. The work consisted in design and construction of the wind-tunnel parts, project managing including purchases and contact with subcontractors as well as the measurements and analysis of the flow quality when the construction work was finished.

Paper 3. Most of the measurements of the flow quality were performed by the respondent but some measurements (total pressure and temperature) were performed by Msc. Valeria Durañona. The respondent performed the analysis of the experimental data.

Paper 4. This paper also appears in Dr. Jens M. Österlund's thesis under a somewhat different name and content. The paper has been extended and rewritten. The measurements were carried out by Dr. Jens M. Österlund. The analysis of the experimental data was equally shared between Dr. Jens M. Österlund and the respondent. The respondent performed the extended analysis contained in the revised version of the paper. The respondent presented this work at the 8th European Turbulence Conference, Barcelona, Spain, 2000, and a written contribution was included in the conference proceedings.

Paper 5. The measurements were performed by Dr. Jens M. Österlund and the respondent performed the analysis of the experimental data. The theoretical analysis was performed together with Prof. Arne V. Johansson. The main part of this work was presented as an invited talk at the IUTAM Symposium on Reynolds number scaling in turbulent flow, Princeton, USA, 2002 by Prof. Arne V. Johansson.

Paper 6. This work was a collaboration with Prof. Yoshiyuki Tsuji from Nagoya University, Japan who for this purpose visited KTH in July 2002. The original ideas came from Prof. Tsuji who together with the respondent analyzed the experimental data. The measurements were performed by Dr. Jens M. Österlund. The respondent presented this work at the IUTAM Symposium on Reynolds number scaling in turbulent flow, Princeton, USA, 2002.

Paper 7. This work was made in collaboration on equal terms with Msc. Olle Törnblom. It was presented at the 9th European Turbulence Conference, Southampton, UK, 2002 by Msc. Olle Törnblom and at the 11th International symposium on application of laser techniques to fluid mechanics, Lisbon, Portugal, 2002 by the respondent, with written contributions to the conference proceedings.

Paper 8. Same as for paper 7 with the exception that the major part of the writing was done by Msc. Olle Törnblom and the simulations were performed by Lic. Johan Gullman-Strand. Parts of the work was presented at the 9th European Turbulence Conference, Southampton, UK, 2002 by Msc. Olle Törnblom and at the 11th International symposium on application of laser techniques to fluid mechanics, Lisbon, Portugal, 2002 by the respondent, with written contributions to the conference proceedings.

Contents

CHAPTER 1

Introduction

The development of tools enabling measurements of aerodynamic forces, *i.e* forces exerted on solid bodies by fluids, such as wind-tunnels, are closely related to the development of heavier than air flying objects, the so called aerodynes. Man has dreamed of flying for a very long time. Most of the early attempts made were based on observations of birds in flight and therefore involved flapping wings, the so called ornithopters. These early attempts were all failures, except perhaps for Daedalus and his son Icarus who managed to take off and escape from the prison tower. Sadly Icarus flew to close to the sun with for us known consequences. In the late 15th and early 16th century Leonardo da Vinci was involved in creating flying machines but all his attempts were based on ornithopters and they failed. However, he also made other studies of fluids in motion, *e.g.* of water flowing past bridge pillars in rivers. This illustrates that the first facility used for flow studies was the nature itself. The unpredictable behaviour of nature later lead to the need for more controlled environments where studies of fluid motion could be performed.

In the 18th century a deeper understanding of the subject of aerodynamics was still lacking, although many studies were made, including measurements of aerodynamic forces. During these early experiments it was found that the force exerted by a fluid on a solid body was a function of the relative speed between the fluid and the body. This understanding lead to the fundamental principle on which all flow devices are based, namely that one can either move the body through the air or keep the body still and move the air, of which the second option is used in wind-tunnels. The first, and simplest, attempts were to make use of the natural wind. It was though abandoned because of the unreliable behaviour of the wind source, with varying speed and direction. The next step was to use a whirling arm, with the model (solid body) mounted at the end of an arm driven by a falling weight, to produce the relative speed between the model and the fluid. Robins, one of the earliest experimentalists in this field found in the 18th century that the relationship between body shape, orientation and flow was much more complex than predicted by the theories previously used.

It was not until the early 19th century that systematic investigations of lift and drag of airfoils were made. Cayley used a whirling arm to perform

such studies and from the results he found he made a small unmanned glider that is believed to be the first successful heavier than air machine. He also concluded that the wings should be fixed, and not flapping, and that the thrust should be produced by some other auxiliary power source. This, however, did not mean the end of the ornithopters. Many efforts have since been made to achieve bird-like flight resulting in nothing but a few good laughs watching old newsreels. However, nowadays there are actually small and light unmanned flying ornithopters driven by rubber band motors.

In the late 19th century it became apparent that the whirling arm was not the optimum tool for aerodynamic studies. A major drawback beside the rotation effects is that the model keeps flying into its own wake. This is not good since the chaotic motion of the fluid (turbulence) in a wake negatively affects the behaviour of the model. Instead wind-tunnels were developed where the model is still and the airflow, usually produced by a fan, passes by the model. The Wright brothers were among the first to understand the usefulness of wind-tunnels in aerodynamic design. They started out by measuring the aerodynamic forces in natural wind using a balance to quantify the effect of camber on lift. They soon found this method inadequate and started doing experiments using a bicycle to achieve the relative difference in velocity between the model and the air. The data they collected encouraged them to continue but instead using a wind-tunnel. They started with a simple tunnel but soon build a more sophisticated one including screens and honeycomb for better flow quality in the test section where the measurements are made. However, they made one error locating the fan at the tunnel inlet which resulted in a swirling flow in the test section. With this tunnel they could finally solve the handling problems of their No. 3 glider in 1902 and the year after they added a 12 hp engine and two counter rotating propellers for their famous 1903 Wright flyer. Next year (2003) there will be many celebrations, conferences and meetings celebrating the 100th anniversary of this event.

The impact of the Wright brothers flying machine was big and an understanding of the importance of wind-tunnels on aircraft development was growing, especially in Europe where government-founded laboratories started building large wind-tunnel facilities till the beginning of world war I in 1914. It was during this era that the two major types of wind-tunnels were developed. The open circuit tunnel or Eiffel tunnel, named after the famous French engineer, and the closed return circuit tunnel or the Prandtl (Göttingen) tunnel, that is named after Prandtl and the German university where it was first built.

There are many ways to classify wind-tunnels. Here I will shortly recapitulate some of the most common ones.

Wind-tunnels may be categorized by the kind of fluid it operates with. As the name wind-tunnel indicates, one commonly uses air but there are also tunnels where water or oil are used. Besides air sometimes other gases are used

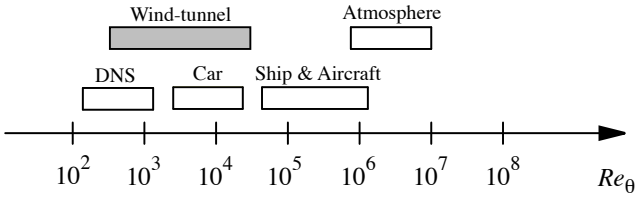

FIGURE 1.1. A sketch of the Reynolds number for different applications. (From Österlund (1999*b*) with permission.)

with the intended purpose of giving the tunnel more favorable properties. The reason for choosing a specific fluid may vary but one reason can be to maximize the Reynolds number. The Reynolds number, named after the famous British scientist who performed experiments on transition in a pipe using dye, (Reynolds (1883)), is a non-dimensional measure of the relative influence of inertial to viscous forces. The Reynolds number can be used as a scaling parameter. Equal Reynolds number in a model experiment and in reality means that the two cases are in some sense dynamically comparable. There are of course other factors that come into play as well but the Reynolds number is an important parameter. Depending on the choice of fluid, the speed of the fluid and the size of the model in the wind-tunnel different Reynolds numbers are achieved. Usually in real applications the Reynolds number is very large. Larger than what is achievable in most wind-tunnel tests, see figure 1.1. The most common choice of a fluid is air and the flow facilities described in this thesis all use air. For a given fluid, the Reynolds number may be increased by the use of larger models or faster test section speeds.

The speed of the air in the test section is common for classifying wind-tunnels. We have *e.g.* hypersonic, supersonic, transonic and subsonic wind-tunnels where the three first groups include wind-tunnels with very high speeds around or above the speed of sound where the compressibility of the air becomes important. The tunnels at the Department of Mechanics are nowadays all subsonic, *i.e.* with speeds well below the speed of sound. Subsonic tunnels may in turn be divided into high-speed and low-speed wind-tunnels and the tunnels referred to in this thesis are of the low-speed type that typically have maximum test section speeds below 100 m/s.

Another way to categorize wind-tunnels are by the intended purpose of use. There are *e.g.* smoke tunnels for flow visualization, automobile tunnels for testing cars, trucks etc, that often have moving floors to simulate the road. Remember that the car is still so the road has to move instead. There are meteorological-environmental tunnel to simulate earth boundary layers which are used to study flow around buildings etc. There are also low-turbulence

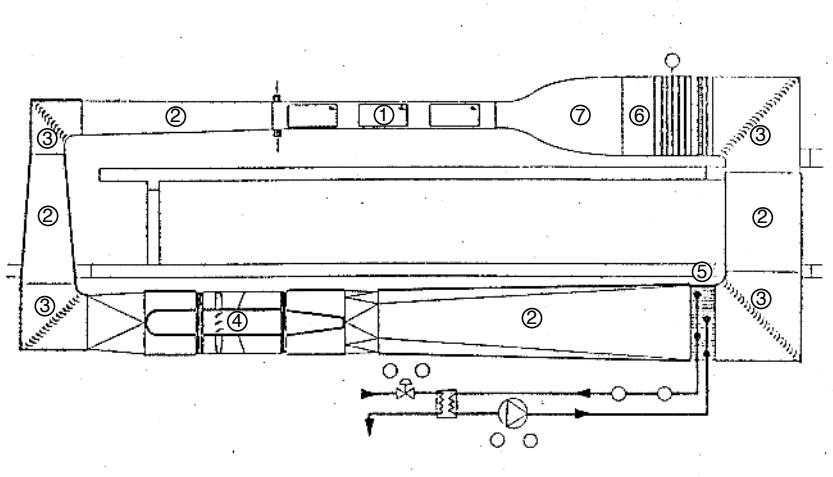

FIGURE 1.2. The MTL wind-tunnel at the Department of Mechanics, KTH.

tunnels that are used to study the fundamental physics of moving fluids. The tunnels treated in this thesis are of this last mentioned type.

The low-turbulence tunnels are characterized by, as indicated in the name, the low level of flow disturbances in the test section. This is achieved by the use of a high contraction ratio, screens and honeycombs which lower the turbulence level and mean flow variations. They are usually of closed circuit type with carefully designed guide-vanes in the corners turning the flow with minimum losses and flow disturbances. They have conservative design of diffusers etc to avoid boundary layer separation. They are also characterized by their relatively high ratio between test section length and cross section area which makes it possible to achieve high Reynolds numbers without high test section speeds. This is advantageous since the typical scales in the flow become larger and thereby easier to measure if the high Reynolds number is achieved by increasing size rather than speed. An example of a low turbulence wind-tunnel is the MTL wind-tunnel, shown in figure 1.2, which is the largest wind-tunnel at the Department of Mechanics, KTH. It has a 7 m long test section with a 1.2×0.8 m^2 cross section area. The main purpose of this wind-tunnel, and the other new wind-tunnel at the department, is to provide a good experimental environment where accurate measurements on transition and turbulence can be performed. Many successful experiments have been performed in the MTL tunnel since its inauguration in 1991. The MTL tunnel was later complemented by a new smaller wind-tunnel with similar characteristics (see figure 1.3) but with the special design feature of expanding corners.

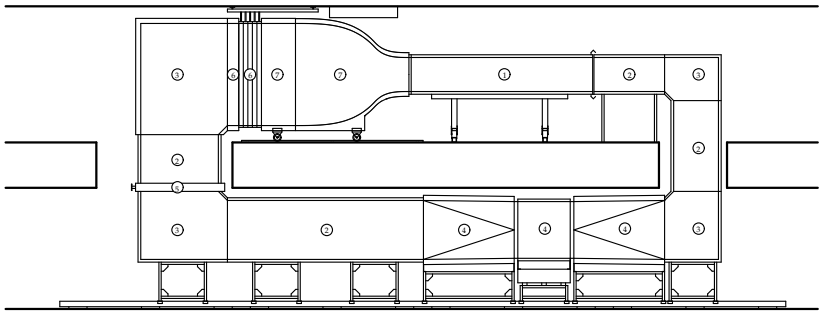

FIGURE 1.3. The new wind-tunnel at the Department of Mechanics, KTH.

One of the experiments performed in the MTL tunnel was that by Jens M. Österlund (see Österlund (1999*b*) from which mean flow data are available in a data-base at Österlund (1999*a*)). The measurements were carried out in a turbulent boundary layer on a flat plate mounted in the MTL wind-tunnel. The experimental data collected have been used in this thesis in the three papers, *Flow structures in zero pressure-gradient turbulent boundary layers at high Reynolds numbers, Universality of probability density distributions in the overlap region in high Reynolds number turbulent boundary layers* and *Evaluation of scaling laws derived from Lie group symmetry methods in zero pressure-gradient turbulent boundary layers*. The flat plate boundary layer flow is a simple generic case which describes the flow close to body surfaces. Choosing a flat plate instead of a more complicated body simplifies the analysis and helps to interpret the physical phenomena in such flows. Boundary layer flows have been investigated for a long time and it was Prandtl who in 1904 (see Prandtl (1904)) invented the concept of boundary layers. He found that friction (viscosity) is important only in a layer very close to the body surface. If the Reynolds number is high enough the flow within this layer becomes chaotic or turbulent, *i.e.* a turbulent boundary layer. Most scaling laws derived for this kind of flow deals with infinite, or very high, Reynolds numbers which means that one of the main efforts is to achieve experimental results for as high Reynolds number as possible without compromising the measurement accuracy.

Among the early important work on turbulent boundary layer flow are those of Schultz-Grunow (1940), Ludwieg & Tillman (1950), Klebanoff (1955) and Smith & Walker (1959). There are also important review papers to mention, where a more thorough survey can be found like the classical paper by Coles (1962) and more recently by Fernholz & Finley (1996).

The Österlund experiments were performed at fairly high Reynolds numbers, Re_θ, (based on momentum-loss thickness and free-stream velocity) up to about 30000. There are several other scientific groups currently performing

similar experiments on zero-pressure gradient turbulent boundary layers. For instance, the group of Hassan Nagib at IIT, Chicago, USA, have performed measurements of the streamwise mean velocity component on a flat plate at Reynolds numbers based on momentum-loss thickness up to approximately 70000 (see Hites (1997) and Nagib *et al.* (2002)). Experiments have also been performed in the commercial DNW tunnel in the Netherlands by Hans H. Fernholz's group from TU, Berlin, Germany. They have carried out measurements both directly on the wind-tunnel test section wall and on a separate boundary layer plate, and have achieved Reynolds numbers up to $Re_\theta = 115000$, (see Fernholz *et al.* (1995) and Knobloch & Fernholz (2002)). In Melbourne, Australia, measurements on a wind-tunnel floor were performed in an open tunnel with a 27 m long test section covering a Reynolds number range up to $Re_\theta = 60000$ (see Jones *et al.* (2002)). A problem with the measurements performed by the two latest groups is that the skin friction have not been measured independently. This somewhat limits the usefulness of the experimental data since an independent measurement of the skin friction is often fundamental in the validation of scaling laws. Experiments at extremely high Reynolds numbers ($\sim 10^6$) are currently under preparation by Alexander Smits *et al.* at Princeton University, Princeton, USA. They can achieve such Reynolds numbers by pressurizing the air and thereby increasing its density. The drawback of this method is that the turbulent scales become very small and difficult to resolve. There is also a prospect to build a very large wind-tunnel in Göteborg, Sweden, with very good flow quality and a 30 m long test section. This project goes under the name of the Nordic wind-tunnel and has an aim of enabling zero-pressure gradient turbulent boundary layer experiments at very high Reynolds numbers, (see Wosnik *et al.* (2002)).

The above mentioned measurements are all made with traditional techniques like hot-wire anemometry and Pitot tubes. In hot-wire anemometry a small wire with a diameter of 0.5-5 μm and a length of about 1 mm depending on wire diameter is heated by an electrical current passing through the wire. The wire is then cooled by the passing air and by measuring the amount of power needed to keep the wire temperature constant or the wire temperature (resistance) for a given power input, the flow velocity and temperature can be measured. Pitot tubes measures the total pressure of the passing air and by relating this pressure to the static pressure the flow velocity can be measured.

Kähler *et al.* (2002) have made experiments at fairly high Reynolds numbers ($Re_\theta = 7800$) in a zero pressure-gradient turbulent boundary layer using Particle Image Velocimetry. The above mentioned techniques gives mean or time resolved velocity data but this technique enables instantaneous views of the flow field in a plane giving two or three velocity components. PIV is a fairly young measurement technique, invented in the 1980th and still under considerable improvement but it will become more widely used in boundary layer kind of flows in the future. It is especially useful when flow separation

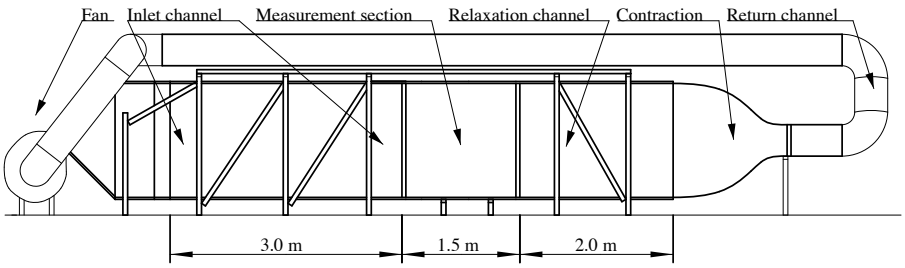

FIGURE 1.4. The flow facility used in the plane asymmetric diffuser measurements.

is present because it yields both direction and absolute value of the velocity. Separated turbulent boundary layer flow has been studied using PIV by *e.g.* Angele (2002).

During the last decade or so, also important numerical simulation work have been made on turbulent boundary layer flow. The first direct numerical simulation was performed by Spalart (1988), who achieved a Reynolds number of $Re_\theta = 1410$. More recently other contributions have been made including also simulations with adverse pressure gradients, see *e.g.* Spalart & Coleman (1997), Na & Moin (1998) and Skote *et al.* (1998). The fast advances made in computer processing speed decreases the gap in Reynolds number between direct numerical simulations and wind-tunnel experiments although at present date this gap is still rather large, see figure 1.1. Martin Skote (private communication) has calculated the time needed to perform a direct numerical simulation of a zero pressure-gradient boundary layer with $Re_\theta = 10000$ using all processors at the new Earth Simulator in Japan and found that it could be done in about six month. It would be very important if such a simulation could be performed, because the Reynolds number is high enough to significantly contribute in solving still open issues (*e.g.* the log-law vs. power-law behaviour of the streamwise mean velocity in the overlap region).

There are turbulent flows that are better studied in other measurement facilities than the all purpose wind-tunnel. It can be experiments where the pressure-drop will be so high that the fan, which is usually axial in a wind-tunnel, cannot deliver a high enough pressure increase for the experiments to be performed. In such cases a flow facility more suited for the particular experiment has to be built. In the early stages of a project involving flow measurements and control in a plane asymmetric diffuser, the intention was to perform the experiments in the newly built low-speed wind-tunnel, which is described in the paper *Design and evaluation of a low-speed wind-tunnel with expanding corners*, in this thesis. Due to some limitations of this all purpose wind-tunnel, like the pressure increase capacity of the fan and the limiting aspect ratio that could be achieved in the test section, the experiment

could not be successfully performed. Instead it was decided that a new flow facility (wind-tunnel), see figure 1.4, specifically designed for measurements in the plane asymmetric diffuser geometry, had to be built. This flow facility is driven by a centrifugal fan which delivers enough pressure for the experiments to be performed at the intended Reynolds number of 2000 based on the friction velocity and the inlet channel height.

Most measurements were performed using optical techniques like Particle Image Velocimetry and Laser Doppler Velocimetry which involves seeding particles, in this case from smoke. A return circuit was made to allow the smoke to be more evenly distributed in the test section and prevent the lab from being filled with smoke. The results from these measurements and comparisons with results obtained in simulations are presented in two papers in this thesis, *Measurements in a plane asymmetric diffuser with 8.5° opening angle. Part I: General flow characteristics* and *Measurements in a plane asymmetric diffuser with 8.5° opening angle. Part II: Comparison with model predictions for turbulence characteristics*. The plane asymmetric diffuser flow includes many interesting flow features, such as an adverse pressure gradient, flow separation, locally high values of turbulence intensity and anisotropy, and streamline curvature, which makes it a complex flow to study despite the simple geometry.

The measurements reported here are not the first in a plane asymmetric diffuser, Obi *et al.* (1993*a*), made measurements in the same kind of flow but with a larger opening angle. They also made some comparisons with $k-\varepsilon$ turbulence models. later they continued their efforts and studied the effect of blowing and suction in a spanwise slit on the inclined wall, (see Obi *et al.* (1993*b*)). In 1997 they made more control investigations and studied the process of momentum transfer in the diffuser (see Obi *et al.* (1997)). The two-dimensionality in their measurements was not quite satisfactory, which encouraged Buice & Eaton (2000) to perform new measurements in the same geometry. Those measurements were intended as reference data for a Large Eddy Simulation performed by Kaltenbach *et al.* (1999). To achieve better two-dimensionality of the mean flow they increased the aspect ratio of the plane asymmetric diffuser.

There has also been many efforts to test turbulence models in this demanding flow. Many of the features typical of this flow, as those mentioned above, are very difficult to predict in a simulation with turbulence models. This makes it a useful test case for turbulence model testing and development. Some examples of work in this field are Hellsten & Rautaheimo (1999), Apsley & Leschziner (1999), Gullman-Strand *et al.* (2002) and Kaltenbach *et al.* (1999). The models tested range from simple $k-\varepsilon$ models to LES, most with moderate success. To be able to learn more about what makes all these models fail in predicting some of the flow features it is important to have a complete set of experimental data for comparisons. However, in all the experiments mentioned above only the velocity components in the streamwise and wall-normal directions were measured. In the separated flow region close to the inclined

wall of the diffuser the amount of experimental data available is also limited. Therefore it was decided to perform new measurements using optical measurement techniques which are very suitable for measurements in separated flows. The opening angle was also changed to 8.5° from the previously used 10° to achieve a flow with a somewhat smaller separated region.

The purpose of these new measurements is to produce a complete data-base including experimental data for all three velocity components. This data-base will be made available for use by turbulence modelers and for comparisons with large eddy and direct numerical simulations. Finding methods of controlling the flow and eliminating the separation bubble is also included in the project. Limited control work have been done by applying a spanwise row of vortex generators which successfully eliminated the separation bubble. More advanced control methods will be tested in the future (see section 4)

The effort of understanding the flow phenomena in duct and diffuser flows and especially achieving efficient control of such flows in terms of eliminating separation and minimizing the pressure drop has increased recently. This kind of flow is very common in engineering and industrial application ranging from ventilation systems, through aircraft air intakes to hydro power plant draft tubes and many other cases. Optimizing these systems can lead to huge gains in energy saving and also improve the efficiency and prolong the expected lifetime of an apparatus by *e.g.* minimizing flow induced vibrations. Although much work has been done on internal flows there is still much more work to be done before a complete understanding of this flow is obtained.

CHAPTER 2

Basic concepts in wall-bounded shear-flows

2.1. Navier-Stokes and Reynolds equations

In the fluid flow cases treated in this thesis the flow is governed by the incompressible Navier-Stokes and continuity equations. Claude Louis Marie Henri Navier was born i Dijon, France in 1785 and died in Paris, France in 1836. Navier, once a student of Fourier, derived the Navier-Stokes equations for incompressible flow in 1821-1822 modifying the Euler equations. Without understanding the concept of shear-stress he instead took into account, what he considered as, forces between the molecules in the fluid. George Gabriel Stokes was born in Skeen, Ireland in 1819 and died in Cambridge, England in 1903. Stokes derived the Navier-Stokes equations in 1845 without knowing that these equations already were derived by Navier. Although he found out before publishing he decided that he had derived the equations in a sufficiently different manner compared to Navier and that his work was still worth publishing.

The incompressible Navier-Stokes equations and the continuity equation read

$$\frac{\mathrm{D}U_i}{\mathrm{D}t} = -\frac{1}{\rho}\frac{\partial P}{\partial x_i} + \nu\frac{\partial^2 U_i}{\partial x_j^2} \tag{2.1}$$

$$\frac{\partial U_i}{\partial x_i} = 0 \tag{2.2}$$

where U_i is the velocity vector, P is the pressure, t is the time, x_i is the spatial vector, ρ is the density and ν is the kinematic viscosity of the fluid. The material time derivative can be written as

$$\frac{\mathrm{D}U_i}{\mathrm{D}t} = \frac{\partial U_i}{\partial t} + U_j\frac{\partial U_i}{\partial x_j} \tag{2.3}$$

For turbulent flows it is often useful to divide the velocity vector and pressure into a mean and a fluctuating part. This division is referred to as the Reynolds (1895) decomposition, after Osborne Reynolds (1842-1912), and for the velocity vector and the pressure it reads

$$U_i(x_i,t) = \overline{U}_i(x_i) + u_i(x_i,t), \tag{2.4}$$

$$P(x,y,z,t) = \overline{P}(x_i) + p(x_i,t), \tag{2.5}$$

where the bar denotes averaged quantity and small letter denotes the fluctuating part. For the Reynolds decomposition to make sense the flow has to be steady, *i.e.*

$$\frac{\partial \overline{U}_i}{\partial t} = 0, \tag{2.6}$$

or varying on a time scale that is much larger than the time scales of the turbulence. Introducing this decomposition into the Navier-Stokes equations and averaging results in the Reynolds averaged equations which together with the continuity equation read

$$\overline{U}_j \frac{\partial \overline{U}_i}{\partial x_j} = -\frac{1}{\rho}\frac{\partial \overline{P}}{\partial x_i} + \nu \frac{\partial^2 \overline{U}_i}{\partial x_j^2} - \frac{\partial \overline{u_i u_j}}{\partial x_j}, \tag{2.7}$$

$$\frac{\partial \overline{U}_i}{\partial x_i} = 0 \tag{2.8}$$

where $-\rho\overline{u_i u_j}$ is the Reynolds stress tensor. This quantity dominates the momentum transfer in most parts of turbulent flows. It also introduces six more unknowns into the four equations represented by 2.7 and 2.8, and thereby the problem of closure that we also refer to as the turbulence modeling problem.

2.2. Turbulent boundary layer flow

One of the flows studied in this thesis is the incompressible turbulent zero pressure-gradient boundary layer flow. The governing equations for this flow can be obtained by introducing the boundary layer approximations, which are constant pressure in the wall-normal direction and zero streamwise diffusion, into the Reynolds averaged equations. If we introduce the mean and fluctuating velocities respectively as $U_i = (U(x,y,z), V(x,y,z), W(x,y,z))$ and $u_i = (u(x,y,z,t), v(x,y,z,t), w(x,y,z,t))$ into the Reynolds averaged equations we obtain

$$\overline{U}\frac{\partial \overline{U}}{\partial x} + \overline{V}\frac{\partial \overline{U}}{\partial y} = -\frac{\partial \overline{uv}}{\partial y} + \nu \frac{\partial^2 \overline{U}}{\partial y^2} \tag{2.9}$$

$$\frac{\partial \overline{U}}{\partial x} + \frac{\partial \overline{V}}{\partial y} = 0 \tag{2.10}$$

where the spanwise direction, z, is assumed to be homogeneous. The boundary conditions are

$$\overline{U}(x, y=0) = 0, \tag{2.11}$$

$$\overline{V}(x, y=0) = 0 \text{ and} \tag{2.12}$$

$$\overline{U}(x, y\to\infty) = U_\infty. \tag{2.13}$$

Unfortunately, it is not possible to solve this set of equations since there are more unknowns than equations. This is the closure problem and further information on the Reynolds shear-stress relating it to the mean flow is needed to solve (close) the problem.

The turbulent boundary layer may be said to be represented by two distinctly different governing length scales, representing characteristic scales for the boundary layer thickness itself and for a thin inner region where viscous stresses play an important role. Similarity solutions can be searched for in these inner and an outer layers (see Millikan (1938)). These solutions are then matched together in a region in between the two layers where both similarity solutions are valid. For the inner layer we have the governing length scale, $l_* = \nu/u_\tau$ where $u_\tau = \tau_w/\rho$ is the friction velocity formed using the wall shear-stress, τ_w, and the density, ρ. The non-dimensional wall-distance then reads $y^+ = y/l_*$. A generalized form for the mean velocity and Reynolds shear-stress in the inner layer can be written as

$$\frac{\overline{U}}{u_\tau} = f(y^+), \tag{2.14}$$

$$-\frac{\overline{uv}}{u_\tau^2} = g(y^+). \tag{2.15}$$

For the outer layer the governing length scale is some measure of the boundary layer thickness, here called δ. This measure could be *e.g.* δ_{99} which is the wall-distance where the velocity has reached 99% of the free-stream velocity, the displacement thickness, δ_*, defined as

$$\delta_* = \int_0^\infty \left(1 - \frac{\overline{U}}{U_\infty}\right) \mathrm{d}y \tag{2.16}$$

(the distance which the streamlines are deflected due to the presence of a solid wall), the momentum-loss thickness, θ, defined as

$$\theta = \int_0^\infty \frac{\overline{U}}{U_\infty}\left(1 - \frac{\overline{U}}{U_\infty}\right) \mathrm{d}y \tag{2.17}$$

(if multiplied by ρU_∞^2 equal to the loss of momentum in a boundary layer compared to potential flow), or the Clauser-Rotta length defined as $\Delta = \delta_* U_\infty/u_\tau$. The non-dimensional wall-distance in outer scaling reads $\eta = y/\delta$ and the generalized form for the mean velocity defect and Reynolds shear-stress respectively in the outer layer can be written

$$\frac{U_\infty - \overline{U}}{u_\tau} = F(\eta), \tag{2.18}$$

$$-\frac{\overline{uv}}{u_\tau^2} = G(\eta). \tag{2.19}$$

Alternatively, we may regard 2.18 as a first order approximation in an expansion of $\overline{U}/U_\infty$ in the small parameter $\gamma = u_\tau/U_\infty$ (*i.e.* $\overline{U}/U_\infty = 1 - \gamma F(\eta) + O(\gamma^2)$). The matching between the layers is achieved, assuming there is a large enough Reynolds number so that $l_* \ll y \ll \delta$, by letting $y^+ \to \infty$ and $\eta \to 0$ simultaneously.

The turbulent boundary layer problem has been investigated theoretically and experimentally since Prandtl (1904) defined the boundary layer. Especially the matching of the two layers has received much attention ever since. In recent years there have been a large debate on whether the classical theory is valid or not. Some of the early important work, in chronological order, are the work by von Kármán (1921, 1930), Prandtl (1927, 1932) and Millikan (1938). However this field of research have been active ever since and Rotta (1950, 1962), Coles (1956), Clauser (1956) and more recently *e.g.* Barenblatt (1993); Barenblatt & Prostokishin (1993), George *et al.* (1997), Zagarola *et al.* (1997), Österlund *et al.* (2000) and Perry *et al.* (2001) have all made important contributions.

2.3. Closure problem in turbulence models

In the field of numerical simulations the closure problem is usually dealt with assuming a simple relationship involving the concept of mixing length first introduced by Prandtl (1927). The mixing length in inner scaling is related to the Reynolds shear-stress and the mean flow gradient as

$$-\overline{uv} = (l^+)^2 \left(\frac{\mathrm{d}\overline{U}^+}{\mathrm{d}y^+} \right)^2 , \tag{2.20}$$

where $l^+ = \varkappa y^+$ is the mixing length. To account for the wall, a damping function can be applied see *e.g.* van Driest (1956). The Prandtl mixing length is based on the Boussinesq (1877) hypothesis which connects the Reynolds stress tensor, $\overline{u_i u_j}$, through the anisotropy tensor, a_{ij}, to the mean rate of strain tensor, S_{ij} using the concept of turbulent viscosity, ν_T. This may be written as

$$a_{ij} = -2\frac{\nu_T}{K} S_{ij}, \text{ where} \tag{2.21}$$

$$a_{ij} = \frac{\overline{u_i u_j}}{K} - \frac{2}{3}\delta_{ij}, \tag{2.22}$$

$$S_{ij} = \frac{1}{2}\left(\frac{\partial \overline{U}_i}{\partial x_j} + \frac{\partial \overline{U}_j}{\partial x_i} \right), \tag{2.23}$$

and where $K = \frac{1}{2} u_i u_i$ is the turbulence kinetic energy and δ_{ij} the Kronecker delta. In the so called two equation models ν_T is commonly expressed as

$$\nu_T = C_\mu \frac{K^2}{\varepsilon} \tag{2.24}$$

where C_μ is a constant and ε the dissipation rate. Transport equations for the turbulence kinetic energy, K, and the dissipation rate, ε, are then solved (see *e.g.* Chou (1945)). Sometimes ε is replaced by the inverse time scale of large eddies, ω, (see *e.g.* Saffman & Wilcox (1974)), or the time scale of large eddies themselves, τ.

However, there are also other turbulence models not based on this simple relationship. The Explicit Algebraic Reynolds Stress Model, EARSM, where the advection and viscous diffusion terms in the transport equation for the anisotropy are neglected, is such a two-equation model with the Boussinesq hypothesis, replaced by a more generalized form of the anisotropy relation, see *e.g.* Gatski & Speziale (1993) and Wallin & Johansson (2000, 2002). The Wallin & Johansson (2000) version of the EARSM model is used in the paper *Measurements in a plane asymmetric diffuser with 8.5° opening angle. Part II: Comparison with model predictions for turbulence characteristics* for comparison with the experimental results in a flow with separation. The simulations were performed by Johan Gullman-Strand. There are also more accurate models like Differential Reynolds Stress Models, DRSM, without the above simplifications of the anisotropy transport equation. This level of modeling may be necessary to accurately capture the plane asymmetric diffuser flow, but it also requires a larger computational effort.

2.4. Basics of Lie group symmetry methods

Recently a new way of achieving scaling laws in turbulent shear-flows has been investigated by Oberlack (2001*a*). Exact solutions, or invariants, to differential equations are here obtained through a method based on Lie group algebra. Basic descriptions of symmetry methods for differential equations are given in *e.g.* Hydon (2000), Oberlack (2001*a*) and Oberlack (2001*b*). The basic idea of symmetry methods for differential equations is to construct methods of finding transformations of the (ordinary or partial) differential equation that do not change its functional form with the change of variables. That is

$$\mathbf{F}\left(\mathbf{x},\mathbf{y},\mathbf{y}_i\right)=0 \Leftrightarrow \mathbf{F}\left(\mathbf{x}^*,\mathbf{y}^*,\mathbf{y}_i^*\right)=0 \tag{2.25}$$

where $\mathbf{x}$ is the vector of independent variables, $\mathbf{y}$ is the vector of dependent variables, index i denotes all derivatives of order i on $\mathbf{y}$ and $*$ denotes the transformed variables. Concentrating our efforts on Lie group symmetries we have analytic transformations that depend on a continuous parameter, ε (not to be confused with the dissipation rate also denoted by ε). We have

$$S_\varepsilon : \mathbf{x}^* = \phi(\mathbf{x},\mathbf{y};\varepsilon) \quad \text{and} \quad \mathbf{y}^* = \psi(\mathbf{x},\mathbf{y};\varepsilon). \tag{2.26}$$

Furthermore, an important property of the Lie groups is that all linear combinations of distinct symmetry groups, $S_\varepsilon^{(i)}$ also are symmetry groups.

Oberlack (2001*a*) discusses the symmetries of the Navier-Stokes and Euler equations, and analyzes further also the symmetries of the differential equation

(derived *e.g.* by Oberlack & Peters (1993)) for the two-point correlation tensor. The two-point correlation tensor is defined as,

$$R_{ij}\left(\mathbf{x},\mathbf{r};t\right)=\overline{u_i'\left(\mathbf{x};t\right)u_j'\left(\mathbf{x}+\mathbf{r};t\right)} \tag{2.27}$$

where $\mathbf{r}$ is the separation vector. An important feature of analyzing the equation for the two-point correlation tensor, is that we can study essentially inviscid dynamics by restricting attention to separations that give length scales that are negligibly influenced by viscosity, and at the same time, restricting attention to positions in space where the influence of viscosity (*e.g.* through viscous stresses) is negligible. This means that all symmetries from the Euler equations carry over to this equation.

Furthermore, restricting ourselves to plane turbulent shear-flows with all mean quantities dependent only on the wall-normal coordinate, y, leaves us with four symmetries. These symmetries are the two scaling symmetries, $\overline{X}_{s_1}$ and $\overline{X}_{s_2}$, here reduced due to the one-dimensional mean flow, $\overline{U}=\overline{U}(y)$, the traditional Galilean invariance in the streamwise direction, $\overline{X}_{\overline{U}}$, and the spatial translation symmetry $\overline{X}_{\overline{V}}$. Remembering the superposition property of Lie group algebra, we can combine the four symmetries into ,

$$\overline{X}=k_{s_1}\overline{X}_{s_1}+k_{s_2}\overline{X}_{s_2}+k_{\overline{U}}\overline{X}_{\overline{U}}+k_y\overline{X}_{\overline{V}}. \tag{2.28}$$

The four symmetries can then be expressed in a characteristic form (see *e.g.* Oberlack (2001*a*)) which reads

$$\begin{aligned}\frac{\mathrm{d}y}{k_{s_1}y+k_y}=\frac{\mathrm{d}r_{[k]}}{k_{s_1}r_{[k]}}=\frac{\mathrm{d}\overline{U}}{(k_{s_1}-k_{s_2})\overline{U}+k_{\overline{U}}}=\\ =\frac{\mathrm{d}R_{[ij]}}{2(k_{s_1}-k_{s_2})R_{[ij]}}\,,\end{aligned} \tag{2.29}$$

where [ ] means that there is no summation over the indices. By changing the values of the two scaling symmetry constants, k_{s_1} and k_{s_2}, the scaling laws for different shear-flow situations can be derived. Scaling laws derived from Lie group symmetries for the mean streamwise velocity and the two-point correlation function are tested against experimental data in the paper, *Evaluation of scaling laws derived from Lie group symmetry methods in zero pressure-gradient turbulent boundary layers.*

CHAPTER 3

Results

3.1. Wind-tunnel design and calibration

The demand for further experimental facilities at the Department of Mechanics, KTH, lead to the decision to design, construct and build a new low-speed closed return circuit wind-tunnel. There were mainly two factors that contributed to this demand. First, there had been an increase in the number of graduate students at the department requiring wind-tunnel time, and secondly a wish to allow undergraduate students to perform their laboratory exercises in a modern high quality flow facility.

Due to the limiting space available in the laboratory, drastic measures had to be taken to be able to fit a large enough test section for the new wind-tunnel to be interesting for research purposes. The solution was to include the use expanding corners, which decreases the total wind-tunnel circuit length drastically for a given test section length, into the design of the wind-tunnel layout.

The idea of expanding corners, *i.e.* a corner with larger outflow than inflow cross-section area, is not new. Since the beginning of the wind-tunnel era this idea has been tested by numerous researchers *e.g.* Kröber (1932), Collar (1936), Friedman & Westphal (1952) and Wolf (1957). However, all these tests were considered failures, mainly due to the poor design of the turning or guide-vanes and the vast amount of money spent in those days on these facilities which meant that wind-tunnel size was not a limiting factor. After studying these reports it was concluded that expanding corners could be a success if proper care was taken in the design of the guide-vanes.

The first experimental tests using a version of the guide-vane used in the MTL tunnel at KTH are reported in Lindgren *et al.* (1997). Various expansion ratios, *i.e.* the ratio between the outflow and the inflow areas, and vane spacings were tested. The results were very encouraging although the total pressure-loss of the corner increased significantly. This increase was thought to be caused by non-optimum shape of the guide-vanes used. Remember that the vane profile tested was highly optimized for a non-expanding corner configuration. The experiments were therefore complemented with calculations using a cascade code originally made for turbine applications. This code named MISES was

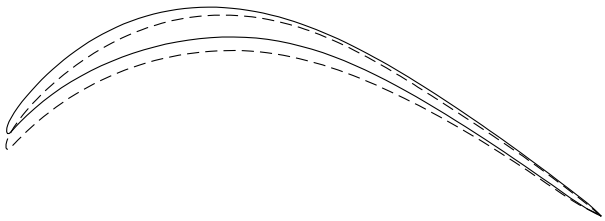

FIGURE 3.1. Solid line: 91L198 optimized for non-expanding corners, $e = 1$ and $\epsilon = 0.3$. Dashed line: L27132B the new vane optimized for expanding corners, $e = \frac{4}{3}$ and $\epsilon = 0.27$.

developed by Youngren & Drela (1991) and is based on the Euler equations for the outer flow region (due to the compressibility effects encountered in turbines) coupled with boundary layer equations for the near-wall regions. One of the main advantages with this code is that there is an inverse optimization tool. Inverse optimization here means that the flow field around the guide-vane profile is decided by the user, through the guide-vane surface pressure distribution, and the code then calculates a shape of the profile that provides a flow field that matches this distribution as close as possible. This has to be done in a step by step process since radical changes causes the code to explode. In this process the shape of the guide-vane slowly changes until the "optimum" pressure distribution giving low pressure-drop, and robustness towards flow angle variations have been achieved.

In figure 3.1 the guide-vane developed for an expansion ratio, e, of 4/3 and a separation between vanes, ϵ, of 0.27 chord lengths is presented (dashed curve) together with the original vane used in the MTL tunnel (solid curve). The total pressure-loss coefficient, defined as

$$\frac{\Delta H}{q_0} = \frac{p_{t0} - \overline{p_{t1}}}{\frac{1}{2}\rho U_0^2} \tag{3.30}$$

where p_{t0} is the total pressure at the corner inlet, $\overline{p_{t1}}$ is the mean total pressure at the corner outlet and U_0 is the mean velocity at the corner inlet, was found to be 0.041 for the new vane whereas the MTL tunnel vane has a total pressure-loss coefficient of 0.036. This slight increase in pressure-loss is somewhat compensated for by the reduced need for diffusers in the wind-tunnel circuit. The development of the new vane for expanding corners is reported in Lindgren *et al.* (1998)

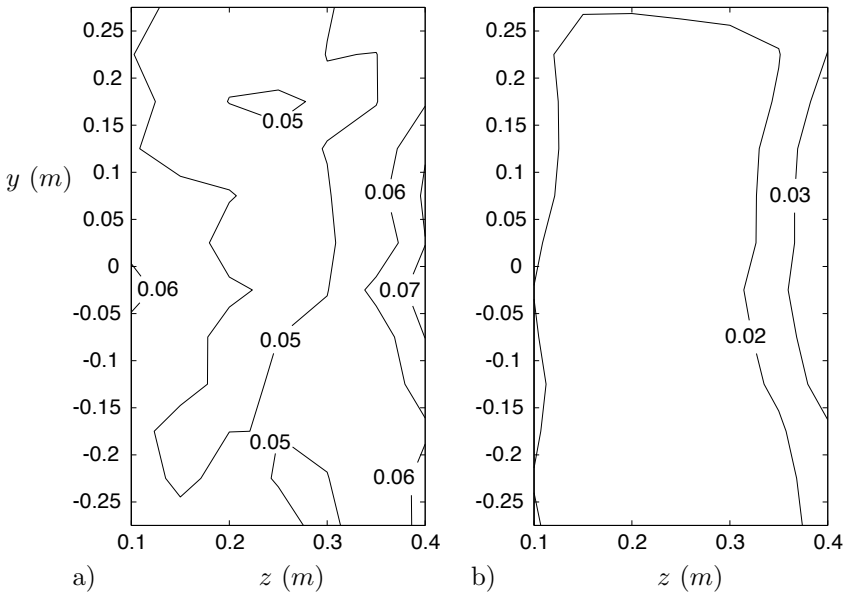

FIGURE 3.2. The streamwise turbulence intensity (in % of the streamwise mean velocity) in the new tunnel at a test section speed of 25 m/s. a) non-filtered data, b) high-pass filtered data with cut-off frequency 20 Hz.

The reason for choosing the rather large expansion ratio of 4/3 is that with a wind-tunnel contraction ratio, *i.e.* the ratio between the largest and smallest cross section areas in the tunnel circuit, of 9 and four corners accommodating all the expansion in one plane the expansion ratio needed in each corner is 4/3. This means that the new wind-tunnel has two-dimensional diffusers that perform slightly worse than three-dimensional diffusers in terms of resistance to separation. A conservative design of the diffusers is therefore needed. The test section is 4 m long with a cross-section area of 0.5×0.75 m^2, and the contraction ratio is 9. A heat exchanger, a honeycomb and 5 screens enhance, together with the large contraction ratio, the flow quality in the test section. The maximum speed in the test section is approximately 45 m/s. The collected knowledge in wind-tunnel design from the construction of the MTL tunnel was used extensively in this project. For instance, the shape of the contraction is identical, the screen wire and mesh sizes are similar and the test section aspect ratio is identical etc. The purpose was not only to benefit from the earlier work but to facilitate relocation of scientific projects between the tunnels and create similar environmental conditions for the experiments.

The flow quality in the test section was extensively investigated and, as an example we may mention that the streamwise turbulence intensity component

($u_{rms}/\overline{U}$) is less than 0.04% and the cross-flow intensity components are less than 0.06%. Furthermore, the total pressure variation ($\Delta\overline{P}(x,z)/(0.5\rho\overline{U}^2$), where $\Delta\overline{P}(x,z)$ is the total pressure difference between a position in the test section and a reference in the stagnation chamber) was found to be less than $\pm 0.1\%$ and the temperature variation less than ± 0.07°C. These values are slightly worse than for the MTL tunnel (see Lindgren & Johansson (2002*b*)), which is expected since the smaller test section cross section area makes the relative influence on the core flow region from the walls larger. In figure 3.2 the turbulence intensity in the streamwise direction is shown for a test section speed of 25 m/s. The figure to the left (a) is the raw data intensity without high-pass filtering of the velocity time signal and the figure to the right (b) is the filtered intensity. The filtering of the data is performed to remove low frequency disturbances not considered as turbulence. These are long wave oscillations stretching around the entire wind-tunnel circuit caused by pressure fluctuations over the axial fan. The design and flow quality measurements are reported in the technical report Lindgren & Johansson (2002*a*).

A similar investigation of the flow quality, as was performed in the new tunnel, was also performed in the MTL tunnel. Measurements of this kind were made when the MTL tunnel was new and are reported in Johansson (1992). However, it was felt that complementary measurements were needed and that they should be reported in an internal technical report, enabling future investigators measuring in the MTL tunnel to refer to this report regarding flow quality statements. The results obtained from the MTL flow quality measurements are reported in Lindgren & Johansson (2002*b*).

The flow quality in the test section of the MTL tunnel was found to essentially agree with the early investigation reported in Johansson (1992). The main difference is that the temperature variation over the test section cross section area was found to be less than ± 0.05°C which is substantially lower than the early findings of ± 0.2°C. This is explained by the improvements in the temperature control system that since have been implemented. The other main results are that the high-pass filtered streamwise turbulence intensity was found to be less than 0.025% and the cross-flow intensities less than 0.035% at a test section speed of 25 m/s. The total pressure variation was found to be less than $\pm 0.06\%$, which actually is slightly better than the result reported in Johansson (1992). This could perhaps be explained by different pressure transducers and truncation of the data in the two investigations.

In figure 3.3 the streamwise turbulence intensity is presented at a test section speed of 25 m/s. Note that if the corners of the measurement area are excluded in the high-pass filtered case (figure 3.3b) the streamwise turbulence intensity would drop below 0.015%. As shown by the difference in figures 3.3a and 3.3b these results are fairly sensitive to the choice of cut-off frequency.

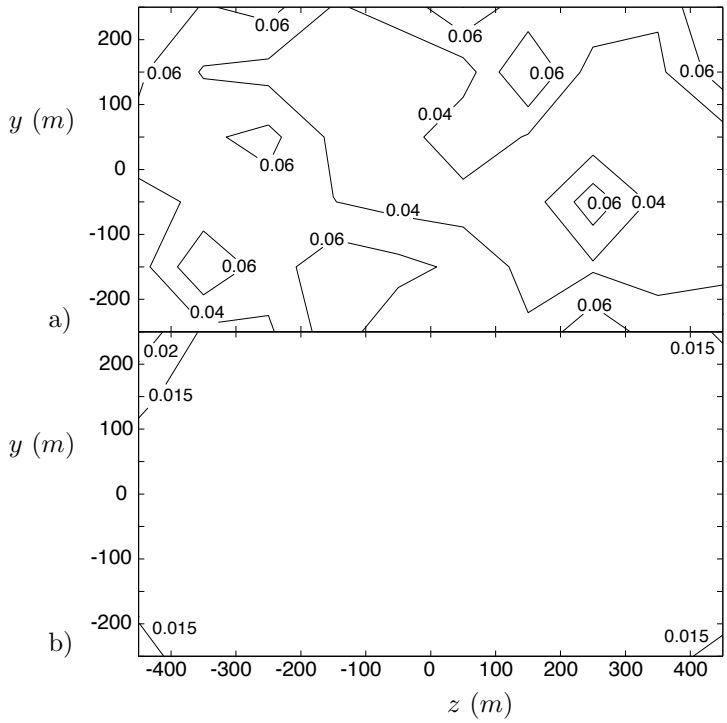

FIGURE 3.3. The streamwise turbulence intensity (in % of the streamwise mean velocity) in the MTL tunnel at a test section speed of 25 m/s. a) non-filtered data, b) high-pass filtered data with cut-off wave length of 2 m.

This choice is also rather subjective, therefore results both for filtered and non-filtered data are presented in the report.

3.2. Evaluation of turbulent boundary layer data

The zero pressure-gradient turbulent boundary layer flow have been studied in three papers in the thesis. They are *Flow structures in zero pressure-gradient turbulent boundary layers at high Reynolds numbers*, *Evaluation of scaling laws derived from Lie group symmetry methods in zero pressure-gradient turbulent boundary layers* and *Universality of probability density distributions in the overlap region in high Reynolds number turbulent boundary layers*. The experimental data used in these investigations are taken from the Österlund (1999*b*) data-base.

In the first of these papers flow structures in the near-wall and buffer regions are studied using a combination of a hot-film array MEMS sensor from

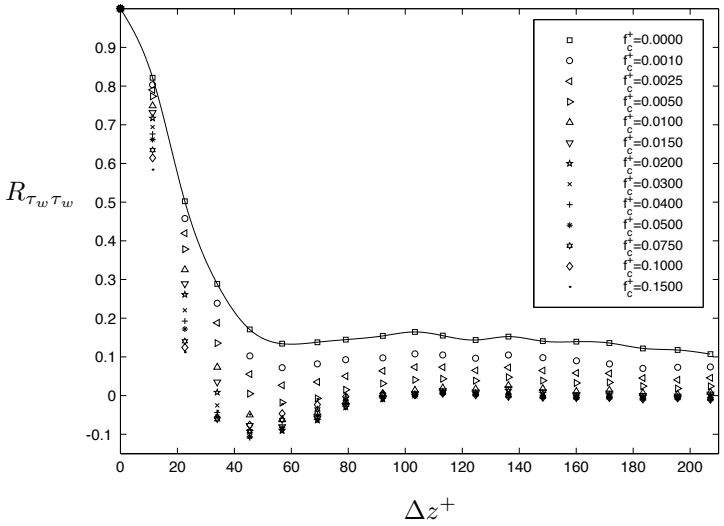

FIGURE 3.4. Determination of the optimum high-pass filter at $Re_\theta = 9500$. Two-point correlation function $R_{\tau_w\tau_w}(\Delta z^+)$ for various degrees of high-pass filtering, (cut-off frequencies given in diagram). The solid line is a spline fit to the unfiltered case.

UCLA/Caltech (see *e.g.* Jiang *et al.* (1996)) and single hot-wires traversed around and above the hot-film array. The hot-film sensor consists of 25 hot-films flush mounted in a spanwise array on the boundary layer plate. The signals from these hot-films was used to calculate the spanwise spacing of near-wall streaks. It is calculated by identifying a local minimum of the correlation function, $R_{\tau_w\tau_w}(\Delta z^+)$, where z^+ is the spanwise coordinate normalized with inner variables. From the raw data, no clear minimum could be identified, see solid line in figure 3.4. The reason is that large scale energetic structures penetrate the near-wall region (so called sweeps) and the contribution to the correlation function from the near-wall streaks are drowned by these dominating large scale structures. This is a problem that increases with increasing Reynolds number since the scale separation then also increases. This kind of phenomenon have been observed both experimentally by Gupta *et al.* (1971) and Naguib & Wark (1992), and recently also in "high" Reynolds number ($Re_\tau = 640$ based on half the channel height and the friction velocity) direct numerical simulations of channel flow by Kawamura *et al.* (private communication). The solution to extract the information from the near-wall streaks is to high-pass filter the wall-shear stress signals eliminating the contribution

from the largest scales. This has been done for many cut-off frequencies (see figure 3.4) and the "largest" minimum in the correlation function was found for a cut-off that corresponds to a typical length of a near-wall streak. The location of the minimum in the correlation function, *i.e.* half the streak spacing, is only slightly affected by the filtering process. With the "optimum" filtering the streak spacing was found to be approximately 96 inner length scales.

It is also worth mentioning that the frequency of occurrence of shear-layer events was found to scale best with a mixed scaling, *i.e.* $t_m = \sqrt{t_i t_o}$ where t_i is the inner and t_o the outer time scale. This result agrees well with the findings for channel flow by Alfredsson & Johansson (1984). More recently Nagano & Houra (2002) investigated time scales in the buffer layer in turbulent boundary layer flow. They found that the Taylor time scale, *i.e.* $t_E = \sqrt{2\overline{u^2}/\overline{(\partial u/\partial t)^2}}$, which is closely related to the mixed timescale, was best, also for adverse pressure-gradient flow.

Scaling laws derived from symmetry methods has recently attracted much attention. The idea is to find transformations of differential equations that leaves the functional form of the equations unchanged in the transformed variables. The advantage of these general methods is that the scaling laws derived are guaranteed to be admissible solutions to the original differential equation studied. From experience one may say that if a solution is admissible it is also likely to appear as a physical solution in nature.

A useful set of symmetries are the Lie group symmetries which are based on a continuous parameter. They are described in detail and applied to various flows by Oberlack *et al.* in *e.g.* Oberlack & Peters (1993); Oberlack (2001*a*). A nice property of the Lie Group symmetries is that any linear combination of the symmetries is also a symmetry.

By assuming parallel wall-bounded shear-flow and essentially inviscid flow dynamics, the four symmetry groups from the evolution equation of the two-point correlation can be written on the characteristic form of equation 2.29 where the ks are scalars to be determined. It is essentially the boundary conditions that impose restrictions on these symmetries but also other factors like viscosity reduce the number of symmetries allowed.

For a zero pressure-gradient boundary layer, we have an overlap region, which is essentially described by inviscid dynamics, and a restriction on free scaling of velocity since u_τ is the governing velocity there. Therefore, the parameters k_{s_1} and k_y in equation 2.29 have to be equal. Integrating the equation then gives the classical log-law but with an extra, higher order, correction term, A^+.

$$\overline{U} = \frac{k_{\overline{U}}}{k_{s_1}} \ln\left(y + \frac{k_y}{k_{s_1}}\right) + B \quad \text{or in inner scaling} \tag{3.31}$$

$$\overline{U}^+ = \frac{1}{\varkappa} \ln\left(y^+ + A^+\right) + B. \tag{3.32}$$

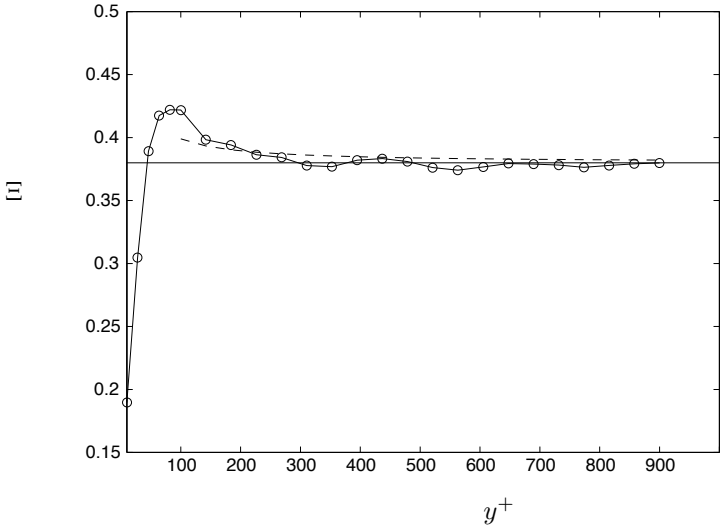

FIGURE 3.5. The diagnostic function Ξ. Solid straight line for classical log-law with $\varkappa = 0.38$ (see Österlund *et al.* (2000)). Dashed curve for modified log-law with $A^+ = 5$.

As shown in figure 3.5, where the diagnostic function

$$\Xi = \left(y^+ \frac{\mathrm{d}\overline{U}}{\mathrm{d}y^+} \right)^{-1} \tag{3.33}$$

should be constant for the classical log-law to be valid, the addition of the $A^+ \approx 5$ constant can be seen as a parameter which extends the logarithmic region towards the wall. However this constant is very small compared to y^+ in the actual overlap region and should primarily be seen as a higher order correction term not affecting the universality and Reynolds number independence of the log-law.

As an interesting note it may be worth mentioning that in the region of strong viscous influence $k_{s_2} = 2k_{s_1}$ (and $k_y = k_{\overline{U}} = 0$ near a boundary) and we simply retrieve the linear profile near the wall.

For the outer, wake, region the governing length scale is given by the boundary layer thickness, δ, which means that the scaling symmetry parameter k_{s_1} must be zero in this region. Integrating the equation yields an exponential

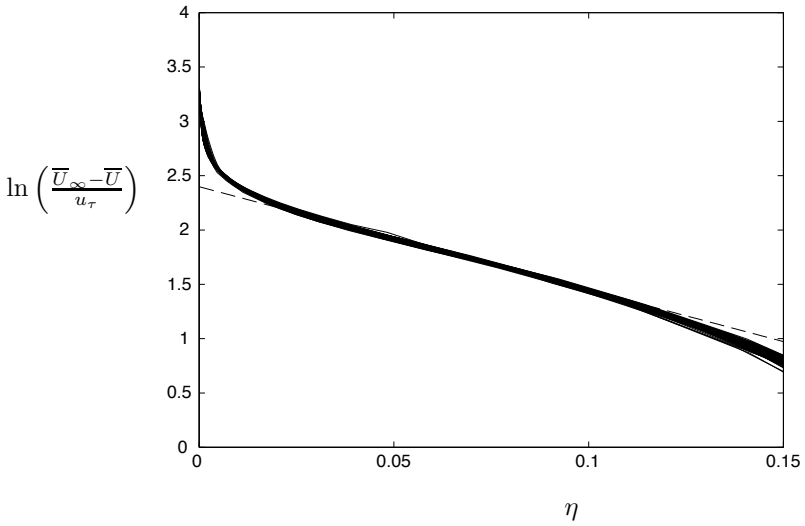

FIGURE 3.6. 70 experimental velocity deficit profiles in outer scaling ($2500 < Re_\theta < 27000$). Dashed line: exponential velocity deficit law with $C_1 = 11$ and $C_2 = 9.5$.

behaviour of the velocity defect.

$$\overline{U} = C_{exp} \exp\left(-\frac{k_{s_2}}{k_y} y\right) + \frac{k_{\overline{U}}}{k_{s_2}} \quad \text{or in outer scaling} \tag{3.34}$$

$$\frac{\overline{U}_\infty - \overline{U}}{u_\tau} = C_1 \exp\left(-C_2 \eta\right). \tag{3.35}$$

In figure 3.6 the exponential velocity defect law, with $C_1 = 11$ and $C_2 = 9.5$, is plotted as a dashed straight line. It fits well to the 70 experimental velocity profiles in a region extending between $0.03 < \eta < 0.12$ corresponding to about half the boundary layer thickness. In the outermost part of the boundary layer there is a deviation of the experimental data away from the exponential velocity defect law. This can in part be explained by the high degree of intermittency encountered here but foremost by the non-parallel flow effects that are found to be important in this region and that are not accounted for in the derivation of the exponential velocity law.

The shape of the probability density distributions (functions), PDFs, in the overlap region was investigated with the purpose of testing if there is a self-similar behaviour in this region. Requiring self-similar PDFs is a very severe restriction since it implies that all higher moments are constant. Looking at the

third and fourth moments (skewness and flatness) we see that they are fairly constant in a region larger than the overlap region as defined by Österlund *et al.* (2000). A similar investigation was performed by Tsuji & Nakamura (1999) for low Reynolds number turbulent boundary layer data ($Re_\theta < 5000$) and they concluded that a larger Reynolds number is needed to find an extended region of self-similar PDFs but that there was still some indications that such a region should exist. This is reasonable since Österlund *et al.* (2000) claims that a Reynolds number larger than $Re_\theta \approx 5000$ is necessary for a universal overlap region to be present.

A sensitive scalar measure of the variation in PDF shapes is the Kullback-Leibler divergence, KLD, (see Kullback (1959)). It is defined as

$$D\left(P\|Q\right) \equiv \sum_{\{s\}} P(s_i) \ln(P(s_i)/Q(s_i)), \tag{3.36}$$

where P and Q are discrete probability density distributions. Here chosen as the experimental data distributions and the Gaussian distribution respectively, (see also Tsuji & Nakamura (1999)). The KLD measure is more sensitive to variations if the two distributions are similar. The choice of the Gaussian distribution as reference distribution is here natural since the experimental distributions are very close to Gaussian in the overlap region. A constant value of the KLD measure means self-similar PDFs.

In figure 3.7 the velocity profile in inner scaling and the KLD measure are shown for a Reynolds number based on momentum-loss thickness of 9700 (top two figures). As we can see the region of constant KLD measure (marked by black squares) is larger than the logarithmic overlap region (marked by black circles) extending further out towards the wake region. In the bottom figure data from all measurements in the Österlund data-base with hot-wire lengths less than 15 viscous length units are plotted together. As seen the collapse is rather remarkable and strongly suggests that the PDFs are indeed self-similar in the overlap region.

As mentioned above the constant KLD region ($180 < y^+$ and $y/\delta_{95} > 0.3$) is somewhat larger than the classical overlap region ($200 < y^+$ and $y/\delta_{95} > 0.15$). Some attempts have been made to establish a new outer limit for the overlap region using the self-similarity of the PDFs but so far no completely satisfying method have been found.

Since the PDFs in the overlap region are very close to Gaussian a truncated Gram-Charlier series expansion is a suitable tool in comparing the different experimental probability density distributions with each other. It is defined as

$$p(\zeta) = c_0 + \phi(\zeta) + \frac{c_1}{1}\phi'(\zeta) + \cdots + \frac{c_n}{n!}\phi^{(n)}(\zeta) \tag{3.37}$$

$$\phi^{(n)}(\zeta) = (-1)^n H_n(\zeta)\phi(\zeta) \tag{3.38}$$

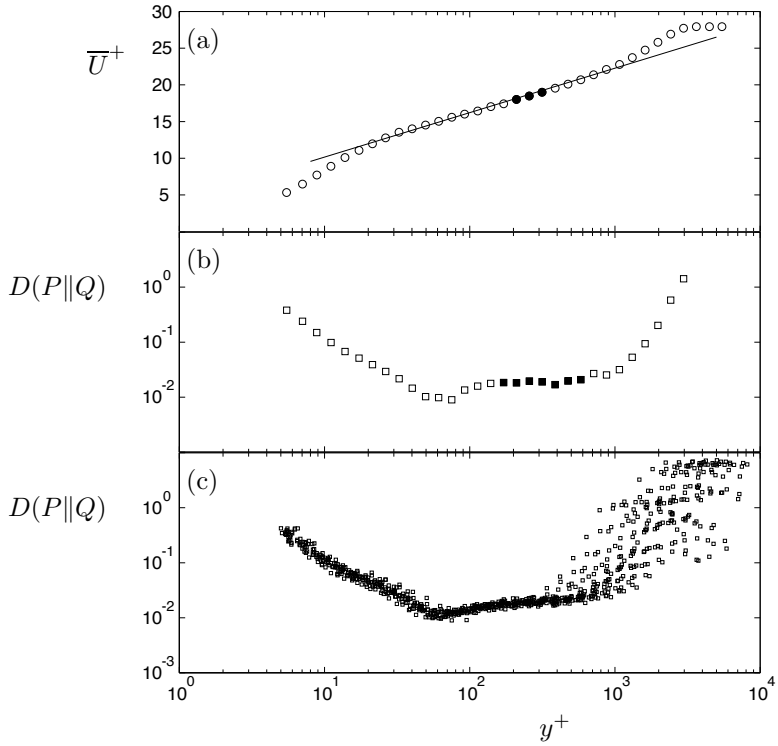

FIGURE 3.7. (Top) Mean velocity profile in inner scaling at $Re_\theta = 9707$. The filled markers correspond to the log-layer, $y^+ > 200$ & $y/\delta_{95} < 0.15$. The solid line represents the log law with $\varkappa = 0.38$ and $B = 4.1$. (Middle) The KLD of the streamwise velocity at $Re_\theta = 9707$. The filled markers correspond to the constant divergence region. (Bottom) The KLD for 18 velocity profiles with wire length $l^+ < 15$ at $2532 < Re_\theta < 12633$.

where ζ is u/u_{rms}, $H_n(\zeta)$ are Hermite functions and $\phi(\zeta)$ is the Gaussian distribution. The coefficients are given by: $c_0 = 1$, $c_1 = c_2 = 0$, $c_3 = -S$ and $c_4 = F - 3$ where S and F are the skewness and flatness factors respectively. Higher order coefficients are related to hyper skewness and hyper flatness in the following way

$$c_5 = -H_S + 10S, \tag{3.39}$$

$$c_6 = H_F - 15F + 30, \tag{3.40}$$

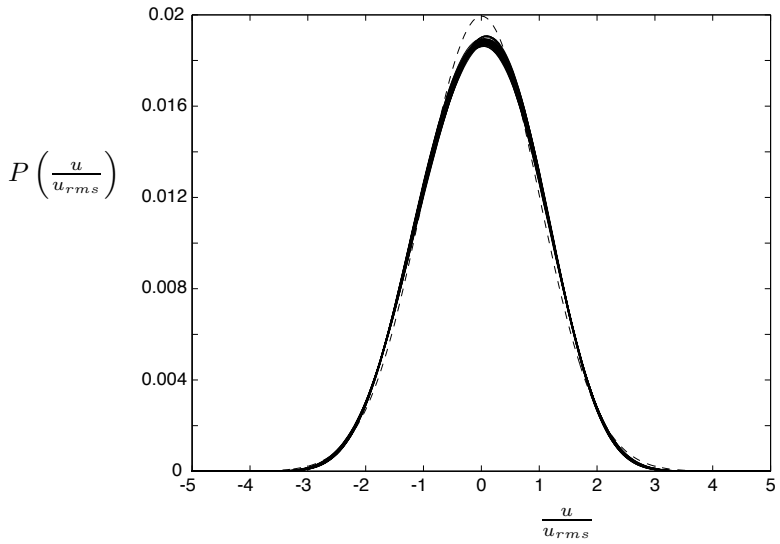

FIGURE 3.8. The probability density functions in the log-layer at $4312 < Re_\theta < 12633$ (57 density distributions). solid lines: Gram-Charlier expansion; dashed line: Gaussian distribution.

where H_S is the hyper skewness and H_F hyper flatness defined as the fifth moment normalized by u_{rms}^5 and the sixth moment normalized by u_{rms}^6.

In figure 3.8 57 Gram-Charlier expanded probability density distributions are plotted together with the Gaussian distribution. The nice collapse further strengthens the hypothesis of self-similar PDFs in the overlap region. Furthermore, plotting the Gram-Charlier coefficients against Reynolds number shows that the variation is small for all moments and that there is no clear Reynolds number trend.

3.3. Plane asymmetric diffuser flow

The flow in an asymmetric plane diffuser with an opening angle of 8.5° was studied primarily using optical measurement techniques. The inlet condition was fully developed channel flow and the Reynolds number based on the friction velocity, u_τ, and the channel height was 2000. This flow case is, as mentioned in chapter 1, very useful for testing new turbulence models since it is a very demanding situation with separated flow, strong pressure-gradient and high turbulence intensity. The purpose of our measurements was to build up a database with all mean and fluctuating velocity components in a plane along the centerline of the diffuser to be used as reference data for turbulence modelers.

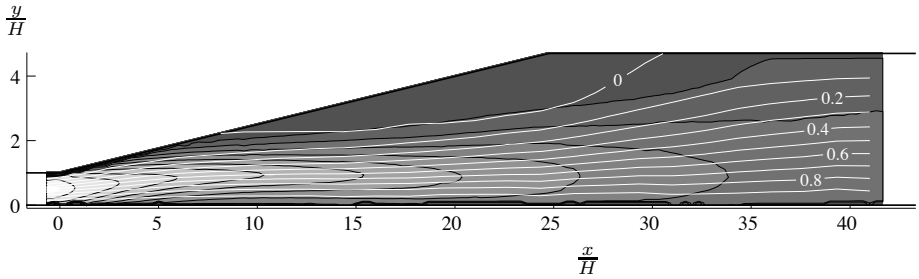

FIGURE 3.9. Streamlines shown as white curves. The stream function is integrated from the inclined wall. Gray-scale background with separating black curves show the speed, with a contour increment of 2 m/s.

Earlier experimental studies of this flow have been made by Obi *et al.* (1993*a*) and Buice & Eaton (2000) but with a slightly larger opening angle (10°). Their case has also been used for comparisons with simulations by *e.g.* Kaltenbach *et al.* (1999) who made a large eddy simulation and Gullman-Strand *et al.* (2002) who made a simulation based on an explicit algebraic Reynolds stress model. The results from a workshop where many turbulence models are tested are reported in Hellsten & Rautaheimo (1999). The results from these simulations are rather mixed. It appears that our case is even more demanding from a simulation point of view since the flow is closer to attached with a smaller opening angle.

In figure 3.9 the streamlines are shown as white curves. The streamline with a stream function value of $\Psi = 0$ is the dividing streamline which separates the region with recirculating flow from the outer flow in a mean sense. The mean separation point is where the upstream end of this dividing streamline meets the wall and the mean reattachment point is where its downstream end meets the wall. In the experiments the separation and reattachment points were found to be at 9 and 31 inlet channel heights downstream of the diffuser inlet, respectively. The gray scale background shown is the speed, *i.e.* $\sqrt{\overline{U}^2 + \overline{V}^2}$ with an increment of 2 m/s between curves. As can be seen in the figure the flow turns towards the inclined wall just downstream of the diffuser inlet and it is deflected back towards the straight wall as soon as the separation bubble starts to develop.

The experimental results are also compared to the results from a simulation using an explicit algebraic Reynolds stress model developed by Wallin & Johansson (2000) with K and ω as the two transported turbulence quantities. These calculations are performed by Johan Gullman-Strand and the scheme

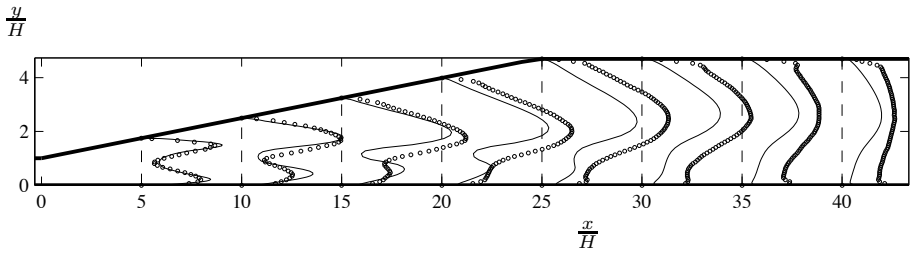

FIGURE 3.10. Turbulence kinetic energy, $K = 1/2(\overline{uu} + \overline{vv} + \overline{ww})$. Solid curve: simulation data. Circles: experimental data.

used is a finite element method with linear base functions both for the velocities and the pressure on a single grid using pressure correction terms. The method is presented in Gullman-Strand (2002).

In figure 3.10 the calculated turbulence kinetic energy is compared to the experimental data. The agreement is very good in the upstream part of the diffuser but there are substantial differences in the downstream part. This is thought to mainly be the result of an under-prediction of the separation bubble size which leads to a less violent flow and thereby less production of turbulence. The mean separation point found in the simulation is 11 inlet channel heights downstream the diffuser inlet, which should be compared to 9 for the experiment and the mean reattachment point was located at $x/H = 27$, which should be compared to 31 in the experiments.

CHAPTER 4

Concluding remark and outlook

Both the newly built and the MTL wind-tunnels have been thoroughly evaluated and although their overall performance was very good there is still room for some improvements. For instance, the settling time of the test section temperature is rather long in both tunnels which is caused by deficiencies in the control loops and the piping. The systems operating the tunnels can also be improved especially regarding their integration with measurement equipment and measurement computers. The flow quality in these tunnels also have to be checked from time to time and the screens have to be cleaned regularly especially now when there is an increase in use of measurement techniques using seeding particles that accumulate in screens and heat exchanger.

The zero pressure-gradient turbulent boundary layer data, measured in the MTL wind-tunnel by Jens M. Österlund, is stored in a data-base which to some extent is available on the internet (see Österlund (1999*a*)). Although the data-base has been extensively used during the last couple of years by Österlund (1999*b*) and others, it is still a useful source of experimental data that can be used for testing and verification of new ideas. During the completion of this thesis, the data-base has been used for testing new scaling laws in the overlap and wake regions, investigating similarity properties of probability density functions in the overlap region and studying near-wall structures in boundary layer flow.

When new scaling laws, derived using Lie group symmetry methods, were tested, it was found that the assumption of parallel flow was appropriate in the overlap region but not in the outer region of the boundary layer. It would certainly be interesting to derive new scaling laws using the same methods but without this assumption. It would also be interesting to include pressure-gradient effects which come in, in a way somewhat similar to non-parallel effects but they will be significant also close to the wall. In Skote & Henningsson (2002) scaling laws are proposed for the inner region for adverse pressure-gradient turbulent boundary layers. They also compared these laws with DNS data. Furthermore, Angele (2002) and Castillo & George (2001) propose scaling laws for the outer region in an adverse pressure gradient turbulent boundary layer. It would be desirable to, via the symmetry group method, find scaling laws for both these regions and compare them to the findings by Skote &

Henningsson (2002), Angele (2002) and Castillo & George (2001). It would also be interesting to make complementary measurements to the existing database with the attention directed towards two-point correlations. Especially the spanwise separation is interesting since this is a homogeneous direction and there is no interference between probes. With such measurements the Taylor's hypothesis used here can be omitted.

The diffuser flow has to be studied further with special attention to the near-wall regions where many features affecting the flow, also in the interior are generated. Capturing the flow in the near-wall regions is therefore essential for a turbulence model to also predict the interior flow field well. The EARSM turbulence model used for comparisons with the experimental data in paper 8 should also include the streamline curvature corrections introduced by Wallin & Johansson (2002). This is especially important in the upstream part of the diffuser where the wall-normal velocity and streamline curvature effects are large. It is plausible that differential Reynolds stress models are necessary to capture this very challenging flow case and with the automated code generation presented in Gullman-Strand (2002), it should be possible to include such models in the future.

The plane asymmetric diffuser project also incorporates control as an important part. This subject has only been touched upon yet with the vortex generator measurements presented in paper 7. There are nowadays many research groups, *e.g.* at the Department of Mechanics, KTH, developing useful control schemes with fast enough feedback to be applicable in a flow like this. The question of sensors and actuators are rather complicated here since the force needed to affect the flow and the wall area of the diffuser are both very large. Some suggestions on actuators are besides the common blowing and suction, piezo electrical flaps, tested in laminar flow by *e.g.* Fredrik Lundell (private communication), wall-jets, inclined vortex generating jets (see *e.g.* Wallis (1960)) and synthetic jets (see *e.g.* Glezer & Amitay (2002)). Another, perhaps more advanced option would be plasma jets (see *e.g.* Lorber *et al.* (2000)). Some of these options may be too complicated and demand too much power input to be feasible in a practical situation, but from a scientific point of view they may still be interesting. The sensor part is even more complicated but traditional wall-wires, and other wall shear-stress sensors based on varying techniques, and miniature speakers to capture pressure fluctuations are some suggestions. However, these aspects of control have to be analyzed further. A good understanding of the basic flow in the diffuser is the first essential step in making the correct choices for the future.

Acknowledgment

I would like to thank my supervisor, Prof. Arne V. Johansson, for accepting me as his student and guiding me through the challenging work facing a graduate student. I am grateful for the funds Arne provided that were necessary to complete this work. I would also like to thank him for critically reviewing this thesis and suggesting improvements to the manuscripts.

I am very thankful towards my friends, office mates and colleagues Jens Österlund and Olle Törnblom, with whom I have cooperated in some projects, for the joy and stimulation in sharing the labour in the otherwise sometimes lonely work situation of a graduate student. We have also shared interesting and exciting moments on regattas with mixed fortunes, above all, of course, due to the unpredictable weather.

I would also like to thank my present and former colleagues with whom I have spent many fun and interesting times both at work and off-work ours. Especially those playing indoor bandy and soccer with whom I have had many hard and challenging encounters.

I would like to thank Prof. Yoshiyuki Tsuji, with whom I worked on one of the papers, for providing interesting views on scaling of turbulent boundary layer flow, and Prof. P. Henrik Alfredsson for his views on the measurements performed in the MTL wind-tunnel.

I wish to thank Mr. Ulf Landén and Mr. Marcus Gällstedt for helping me in designing and manufacturing high quality measurement equipment and wind-tunnel parts that are critical in the achievement of good experimental data.

Finally the Swedish Research Council for Engineering Science (TFR), the Swedish National Board for Industrial and Technical Development (NUTEK) and the Swedish Research Council (VR) are gratefully acknowledged for financial support.

Bibliography

Alfredsson, P. H. & Johansson 1984 Time scales in turbulent channel flow. *Phys. Fluids A* **27** (8), 1974–81.

Angele, K. P. 2002 Pressure-based scaling in a separating APG boundary layer. In *Advances in Turbulence IX* (ed. I. P. Castro, P. E. Hancock & T. G. Thomas), pp. 639–642. CIMNE, Barcelona, Spain.

Apsley, D. D. & Leschziner, M. A. 1999 Advanced turbulence modelling of separated flow in a diffuser. *Flow, Turbulence and Combustion* **63**, 81—112.

Barenblatt, G. I. 1993 Scaling laws for fully developed turbulent shear flows. Part 1. Basic hypotheses and analysis. *J. Fluid Mech.* **248**, 513–520.

Barenblatt, G. I. & Prostokishin, V. M. 1993 Scaling laws for fully developed turbulent shear flows. Part 2. Processing of experimental data. *J. Fluid Mech.* **248**, 521–529.

Boussinesq, T. V. 1877 Essai sur la théorie des eaux courantes. *Mém. Prés. Acad. Sci.* p. 46.

Buice, C. U. & Eaton, J. K. 2000 Experimental investigation of flow through an asymmetric plane diffuser. *Tech. Rep.* TSD-107. Thermo sciences Division, Dep. of Mechanical Eng. Stanford University, Stanford, Ca, USA, Report No.

Castillo, L. & George, W. K. 2001 Similarity analysis for turbulent boundary layer with pressure gradient: Outer flow. *AIAA J.* **39** (1), 41–47.

Chou, P. Y. 1945 On velocity correlations and the solutions of the equations of turbulent motion. *Quart. of Applied Math.* **3**, 38–54.

Clauser, F. H. 1956 The turbulent boundary layer. *Advances Appl. Mech.* **4**, 1–51.

Coles, D. E. 1956 The law of the wake in the turbulent boundary layer. *J. Fluid Mech.* **1**, 191–226.

Coles, D. E. 1962 The turbulent boundary layer in a compressible fluid. R 403-PR. The RAND Corporation, Santa Monica, CA.

Collar, A. R. 1936 Some experiments with cascades of aerofoils. A.R.C. Technical Report 1768. Aeronautical research committee.

van Driest, E. R. 1956 On turbulent flow near a wall. *J. Aero. Sci.* **23**, 1007–1011.

Fernholz, H. H. & Finley, P. J. 1996 The incompressible zero-pressure-gradient turbulent boundary layer: An assessment of the data. *Prog. Aerospace Sci.* **32**, 245–311.

Fernholz, H. H., Krause, E., Nockemann, M. & Schober, M. 1995 Comparative measurements in the canonical boundary layer at $Re_{\delta_2} < 6 \cdot 10^4$ on the wall of the german-dutch windtunnel. *Phys. Fluids* **7** (6), 1275–1281.

Friedman, D. & Westphal, W. R. 1952 Experimental investigation of a 90° cascade diffusing bend with an area ratio of 1.45:1 and with several inlet boundary layers. TN 2668. NACA.

Gatski, T. B. & Speziale, C. G. 1993 On explicit algebraic stress models for complex turbulent flows. *J. Fluid Mech.* **254**, 59–78.

George, W. K., Castillo, L. & Wosnik, M. 1997 Zero-pressure-gradient turbulent boundary layer. *Applied Mech. Reviews* **50**, 689–729.

Glezer, A. & Amitay, M. 2002 Synthetic jets. *Ann. Rev. Fluid Mech.* **34**, 503–529.

Gullman-Strand, J. 2002 Turbulence modeling using automated code generation applied to asymmetric diffuser flow. *Tech. Rep.* 2002:06. Lic. thesis, Dept. of Mechanics, KTH, TRITA-MEK.

Gullman-Strand, J., Amberg, G. & Johansson, A. V. 2002 Study of separated flow in an asymmetric diffuser. In *Advances in Turbulence IX*, pp. 643–646. Southampton, U.K.

Gupta, A. K., Laufer, J. & Kaplan, R. E. 1971 Spatial structure in the viscous sublayer. *J. Fluid Mech.* **50**, 493–512.

Hellsten, A. & Rautaheimo, P., ed. 1999 *Workshop on refined turbulence modelling*. ERCOFTAC/IAHR/COST.

Hites, M. H. 1997 Scaling of high-Reynolds number turbulent boundary layers in the National Diagnostic Facility. PhD thesis, Illinois Institute of Technology.

Hydon, P. 2000 *Symmetry Methods for Differential Equations - A Beginner's Guide*. Cambridge University Press Publisher.

Jiang, F., Tai, Y.-C., Gupta, B., Goodman, R., Tung, S., Huang, J. B. & Ho, C.-M. 1996 A surface-micromachined shear stress imager. In *1996 IEEE Micro Electro Mechanical Systems Workshop (MEMS '96)*, pp. 110–115.

Johansson, A. V. 1992 A low speed wind-tunnel with extreme flow quality-design and tests. *Proc. the 18:th ICAS Congress* pp. 1603–1611.

Jones, M. B., Nishizawa, N., Chong, M. S. & Marusic, I. 2002 Scaling of the turbulent boundary layer at high Reynolds numbers. In *IUTAM symposium on Reynolds number scaling in turbulent flow*. Princeton, University, NJ, USA.

Kähler, C. J., Stanislas, M. & Kompenhans, J. 2002 Spatio-temporal flow structure investigation of near-wall turbulence by means of multiplane stereo particle image velocimetry. In *11th Int. Symp. on Applications of Laser Techniques to Fluid Mech.*. Instituto superior técnico, Center for innovation, technology, and policy research, Lisbon, Portugal.

Kaltenbach, H. J., Mittal, M., Fatica, R., Lund, T. S. & Moin, P. 1999 Study of flow in a planar asymmetric diffuser using large-eddy simulation. *J. Fluid Mech.* **390**, 151–185.

von Kármán, T. 1921 Ueber laminare un turbulente Reibung. *Z. angew. Math. Mech.* pp. 233–252, NACA TM 1092.

von Kármán, T. 1930 Mechanische Aehnlichkeit und Turbulenz. *Nachr. Ges. Wiss. Göttingen, Math. Phys. Kl.* pp. 58–68, NACA TM 611.

Klebanoff, P. S. 1955 Characteristics of turbulence in a boundary layer with zero pressure gradient. TR 1247. NACA.

Knobloch, K. & Fernholz, H. H. 2002 Statistics, correlations and scaling in a canonical, incompressible turbulent boundary layer with $Re_{\delta_2} \leq 1.15 \times 10^5$. In *IUTAM symposium on Reynolds number scaling in turbulent flow*. Princeton, University, NJ, USA.

Kröber, G. 1932 Schaufelgitter zur umlenkung von flussigkeits-strömung. *Ingenieur-Archiv* **3**, 516.

Kullback, S. 1959 *Information theory and statistics*. Wiley, London.

Lindgren, B. & Johansson, A. V. 2002*a* Design and evaluation of a low-speed wind-tunnel with expanding corners. TRITA-MEK 2002:14. Department of Mechanics, KTH.

Lindgren, B. & Johansson, A. V. 2002*b* Evaluation of the flow quality in the low-speed MTL wind-tunnel. TRITA-MEK 2002:13. Department of Mechanics, KTH.

Lindgren, B., Österlund, J. & Johansson, A. V. 1997 Measurement and calculation of guide vane performance in expanding bends for wind tunnels. TRITA-MEK 1997:6. Department of Mechanics, KTH.

Lindgren, B., Österlund, J. M. & Johansson, A. V. 1998 Measurement and calibration of guide-vane performance in expanding bends for wind-tunnels. *Experiments in Fluids* **24**, 265–272.

Lorber, P., McCormick, D., Anderson, T., Wake, B., MacMartin, D., Pollack, M., Corke, T. & Breuer, K. 2000 Rotorcraft retreating blade stall control. In *Fluids 2000 conference and exhibit*, , vol. AIAA 2000-2475. Denver, Colorado, USA.

Ludwieg, H. & Tillman, W. 1950 Investigations of the wall shearing stress in turbulent boundary layers. TM 1285. NACA.

Millikan, C. B. 1938 A critical discussion of turbulent flows in channels and circular tubes. In *Proceedings of the Fifth International Congress of Applied Mechanics*.

Na, Y. & Moin, P. 1998 Direct numerical simulation of a separated turbulent boundary layer. *J. Fluid Mech.* **374**, 379–405.

Nagano, Y. & Houra, T. 2002 Scaling of near-wall structures in turbulent boundary layers subjected to adverse pressure gradient. In *IUTAM symposium on Reynolds number scaling in turbulent flow*. Princeton, University, NJ, USA.

Nagib, H. M., Christophorou, C., Monkewitz, P. A. & Österlund, J. M. 2002 Higher Reynolds number boundary layer data on a flat plate in the NDF. In *IUTAM symposium on Reynolds number scaling in turbulent flow*. Princeton, University, NJ, USA.

Naguib, A. M. & Wark, C. E. 1992 An investigation of wall-layer dynamics using a combined temporal filtering and correlation technique. *J. Fluid Mech.* **243**, 541–560.

Oberlack, M. 2001*a* *Lecture notes from CISM cource on Theories of Turbulence, Udine*. To be published by Springer.

Oberlack, M. 2001*b* A unified approach for symmetries in plane parallel turbulent shear flows. *J. Fluid Mech.* **427**, 299–328.

Oberlack, M. & Peters, N. 1993 *Closure of the two-point correlation as a basis of Reynolds stress models. In So, R., Speziale, C., Launder, B., eds.,* Near wall turbulent flows*, 85–94*. Elsevier Science Publisher.

Obi, S., Aoki, K. & Masuda, S. 1993*a* Experimental and computational study of turbulent separating flow in an asymmetric plane diffuser. In *9th Symp. on Turbulent Shear Flows, Kyoto, Japan, August 16-18*, p. 305.

Obi, S., Ishibashi, N. & Masuda, S. 1997 The mechanism of momentum transfer enhancement in periodically perturbed turbulent separated flow. In *2nd Int. Symp. on Turbulence, Heat and Mass Transfer, Delft, The Netherlands*, pp. 835–844.

Obi, S., Ohizumi, K. & Masuda, S. 1993*b* Turbulent separation control in a plane asymmetric diffuser by periodic perturbation. In *Engineering Turbulence Modeling and Experiments 2*, pp. 3633–642.

Österlund, J. M. 1999*a* http://www.mech.kth.se/~jens/zpg/.

Österlund, J. M. 1999*b* Experimental studies of zero pressure-gradient turbulent boundary-layer flow. PhD thesis, Department of Mechanics, Royal Institute of Technology, Stockholm.

Österlund, J. M., Johansson, A. V., Nagib, H. M. & Hites, M. H. 2000 A note on the overlap region in turbulent boundary layers. *Phys. Fluids* **12**, 1–4.

Perry, A. E., Hafez, S. & S., C. M. 2001 A possible reinterpretation of the Princeton superpipe data. *J. Fluid Mech.* **439**, 395–401.

Prandtl, L. 1904 Ueber die Flüssigkeitsbewegung bei sehr kliner Ribung. In *Verhandlungen des III. Internationalen Mathematiker-Kongress, Heidelberg*, pp. 484–491.

Prandtl, L. 1927 Ueber den Reibungswiderstand strömender Luft. *Ergebn. Aerodyn. Versuchsanst. Göttingen* **3**, 1–5.

Prandtl, L. 1932 Zur turbulenten Strömung in Rohren und längs Platten. *Ergebn. Aerodyn. Versuchsanst. Göttingen* **4**, 18–29.

Reynolds, O. 1883 On the experimental investigation of the circumstances which determine whether the motion of water shall be direct or sinuous, and the law of resistance in parallel channels. *Phil. Trans. Roy. Soc. Lond.* **174**, 935–982.

Reynolds, O. 1895 On the dynamical theory of incompressible viscous fluids and the determination of the criterion. *Phil. Trans. Roy. Soc. A* **186**, 123–164.

Rotta, J. C. 1950 Über die Theorie der Turbulenten Grenzschichten. Mitt. M.P.I. Ström. Forschung Nr 1, also available as NACA TM 1344.

Rotta, J. C. 1962 Turbulent boundary layers in incompressible flow. In *Progress in aeronautical sciences* (ed. A. Ferri, D. Küchemann & L. H. G. Sterne), , vol. 2, pp. 1–219. Pergamon press.

Saffman, P. G. & Wilcox, D. C. 1974 Turbulence-model predictions for turbulent boundary layers. *AIAA Journal* **12**, 541–546.

Schultz-Grunow, F. 1940 Neues Reibungswiederstandsgesetz für glatte Platten. *Tech. Rep.* 8. Luftfahrtforschung, translated as *New frictional resistance law for smooth plates*, NACA TM-986, 1941.

Skote, M. & Henningsson, D. S. 2002 Direct numerical simulation of a separated turbulent boundary layer. *J. Fluid Mech.* **471**, 107–136.

Skote, M., Henningsson, D. S. & Henkes, R. A. W. M. 1998 Direct numerical simulation of self-similar turbulent boundary layers in adverse pressure gradients. *Flow, Turbulence and Combustion* **60**, 47–85.

Smith, D. W. & Walker, J. H. 1959 Skin-friction measurements in incompressible flow. NASA TR R-26.

Spalart, P. R. 1988 Direct simulation of a turbulent boundary layer up to $Re_\theta = 1410$. *J. Fluid Mech.* **187**, 61–98.

Spalart, P. R. & Coleman, G. N. 1997 Numerical study of a separation bubble with heat transfer. *European J. of Mech. B/Fluids* **16**, 169.

Tsuji, Y. & Nakamura, I. 1999 Probability density function in the log-law region of low Reynolds number turbulent boundary layer. *Phys. Fluids* **11** (3), 647–658.

Wallin, S. & Johansson, A. V. 2000 An explicit algebraic Reynolds stress modell for incompressible and compressible turbulent flows. *J. Fluid Mech.* **403**, 89–132.

Wallin, S. & Johansson, A. V. 2002 Modeling streamline curvature effects in explicit algebraic Reynolds stress turbulence models. *Int. J. of Heat and Fluid Flow.* **23**, 721–730.

Wallis, R. A. 1960 A preliminary note on a modified type of air jet for boundary layer control. *Tech. Rep.* C.P. No. 513. Aeronautical Research Council, A.R.C.

Wolf, H. 1957 Messungen im nachlauf eines gleichdruckgitters für 90-umlenkung. *Maschinenbautechnik* **6** (10), 539.

Wosnik, M., George, W. K., Karlsson, R. I. & Johansson, T. G. 2002 The Nordic Wind-Tunnel - proposal to build a large turbulence research facility. In *Advances in turbulence IX*, p. 899. CIMNE, Barcelona, Spain.

Youngren, H. & Drela, M. 1991 Viscous/inviscid method for preliminary design of transonic cascades. In *AIAA, SAE, ASME, and ASEE, Joint Propulsion,Conference, 27th.*.

Zagarola, M. V., Perry, A. E. & Smits, A. J. 1997 Log laws or power laws: The scaling in the overlap region. *Phys. Fluids* **9** (7), 2094–100.